Manuscript Number: wes-2025-131

Title: Failure classification of wind turbine operational conditions using hybrid machine learning

Dear Editor,

We have improved the article ref. wes-2025-131 was extensively revised in accordance with the reviewer's suggestions and comments. We strongly believe that Wind Energy Science would be the most suitable journal for this work. Please find attached the revised manuscript.

General comments from the reviewers. Reviewer 2 emphasised the relevance and motivation of the proposed study, while highlighting the strong potential for wind turbine monitoring. We are grateful for their constructive comments and suggestions, which have been carefully considered to improve the manuscript.

Our general response: This version has been carefully revised to incorporate all the reviewers' suggestions, and we hope it will be suitable for publication in the Wind Energy Science journal. In general, the reviewer's comments were highly appreciated and helped us significantly improve the quality of our manuscript. We are grateful for their consideration and time to review our paper. In the following pages, we provide point-by-point responses to each reviewer's comments. We have highlighted the revised parts in the manuscript in blue.

Yours sincerely, M. R. Machado A De Sousa J. S. Coelho R. Teloli

RC1: 'Comment on wes-2025-131', Anonymous Referee #1, 26 Aug 2025

This paper proposes a hybrid machine learning framework combining feature engineering with classification algorithms to detect operational failures in wind turbines using vibration and environmental data. However, the paper suffers from structural deficiencies and lacks clear motivation. While machine learning approaches for wind turbine fault detection are valuable, this work does not adequately differentiate itself from existing literature or demonstrate sufficient novelty for publication. The experimental design contains several methodological flaws that compromise the reliability of the reported results. I have the following comments on the detailed assessment of these issues:

Answer: We thank the reviewer for the comments and the opportunity to clarify and improve the paper. We carefully addressed each issue pointed out, which certainly helped to improve the quality of our manuscript.

The objective of this work is to propose a hybrid monitoring framework that combines multiple machine learning models and integrates multimodal data, thereby enhancing the interpretability of the Aventa wind turbine fault detection. Unlike conventional single-model or single-source approaches, this hybrid strategy improves cross-domain correlations and environmental variability, enabling reliable monitoring under complex operational conditions. The model employs unsupervised k-means clustering to group data into homogeneous clusters, thereby facilitating pattern recognition without predefined labels, and multiple supervised classification machine learning algorithms for binary or multiclass fault classification. Since different algorithms may perform better under different scenarios and operating conditions, the proposed framework analyzes different machine learning algorithms. It identifies the best-performing model for the applied study case.

Furthermore, within this framework, the proposed relative change damage index introduces a feature normalising and scaling strategy that enhances the comparability of heterogeneous features without requiring predefined baselines. This improves sensitivity to operational deviations and ensures consistent feature interpretation across different sensors. Additionally, the canonical correlation-based feature and sensor selection method evaluates multivariate dependencies between response features and fault classes, providing a physically consistent, data-driven basis for ranking sensor importance. The main contributions of this study are:

- (i) the development of a hybrid ML framework for operational fault assessment combining multiple algorithms and multimodal data,
- (ii) the introduction of a feature relative change strategy for feature normalisation and scaling, and
- (iii) the implementation of a canonical correlation-based feature and sensor selection process.

The proposed model enhances interpretability, scalability, and diagnostic performance. Comparative results across different scenarios confirmed the model's accuracy (85–98%) and stability, validating the methodological distinction in a practical application.

A deeper explanation and demonstration of the hybrid model, along with how our paper differs from previous literature, were included in the introduction.

1. The introduction does not adequately establish a clear research gap or compelling motivation for this work. The authors need to articulate more clearly what distinct advantages their proposed approach offers compared to existing methodologies.

Answer: We thank the reviewer for the comment. In the revised version, we have improved the organisation of the introduction, including references to better emphasise the research gap and the contributions of this work, and to guide readers through past developments in the field.

The objective of this work is to propose a hybrid monitoring framework that combines multiple machine learning models and integrates multimodal data, thereby enhancing the interpretability of the Aventa wind turbine fault

detection. Unlike conventional single-model or single-source approaches, this hybrid strategy improves cross-domain correlations, multiphysics interactions, and environmental variability, enabling reliable monitoring under complex operational conditions. The model employs unsupervised k-means clustering to group data into homogeneous clusters, thereby facilitating pattern recognition without predefined labels, and multiple supervised classification machine learning algorithms for binary or multiclass fault classification. Since different algorithms may perform better under different scenarios and operating conditions, the proposed framework analyzes different machine learning algorithms. It identifies the best-performing model for the applied study case.

Furthermore, within this framework, the proposed relative change damage index introduces a feature normalising and scaling strategy that enhances the comparability of heterogeneous features without requiring predefined baselines. This improves sensitivity to operational deviations and ensures consistent feature interpretation across different sensors. Additionally, the canonical correlation-based feature and sensor selection method evaluates multivariate dependencies between response features and fault classes, providing a physically consistent, data-driven basis for ranking sensor importance. The main contributions of this study are:

- (i) the development of a hybrid ML framework for operational fault assessment combining multiple algorithms and multimodal data,
- (ii) the introduction of a feature relative change strategy for feature normalisation and scaling, and
- (iii) the implementation of a canonical correlation-based feature and sensor selection process.

The proposed model enhances interpretability, scalability, and diagnostic performance. Comparative results across different scenarios confirmed the model's accuracy (85–98%) and stability, validating the methodological distinction in a practical application.

Thus, the distinct advantage of this work lies in its hybridization of ML models and multiphysics data fusion, which together enhance diagnostic accuracy, robustness, and interpretability beyond what existing SHM strategies provide. A deeper explanation and demonstration of the hybrid model, along with how our paper differs from previous literature, were included in the introduction.

- 2. The manuscript contains numerous grammatical errors and inconsistencies that impede readability, for example: **Answer:** We thank the reviewer for the comment. The following actions were incorporated in the revised manuscript.
- o Line 20: Incorrect citation formatting "...those turbines Veers et al. (2023)"- Answer: We revised the reference list.
- o Algorithm 1, Step 1: "Receive structural ... from the time-domain responses"- Answer: Now it reads: "Receive structural response data from the time-domain accelerometer measurements and environmental conditions from the SCADA system."
- o Line 128: ... to capture the most information about the damage ... Answer: We revised this sentence. Now it reads: "Table 1 lists the SCADA data and accelerometers used for monitoring, along with their respective sensor channels and locations. The x-axis captures side-to-side turbine motion, and the y-axis captures fore-aft turbine motion."
- o Undefined abbreviations (RHS, LHS in Figure 4 caption, DT algorithm) Answer: According to the Chicago manual of style, lhs means left-hand side and rhs means right-hand side. We used the standard abbreviations in the caption of Figure 4.
- In the new version of the manuscript, it was substituted with letters as (a), (b), and (c). DT algorithm was defined Decision tree (DT).

3. The statement on line 35 that "unlike traditional methods that rely on hand-crafted features, machine learning enables ..." requires clarification and justification. The shallow machine learning models implemented in this work are fundamentally dependent on hand-crafted features rather than learned representations.

Answer: We thank the reviewer for this comment. We acknowledge that the original statement may have been misleading. We intended to contrast traditional SHM methods, which typically rely on physics-based analytical models or a limited set of manually selected statistical features, with modern data-driven approaches that can automatically process large datasets. We agree that the shallow ML models employed in this study still depend on feature extraction. However, these features are automatically derived from the measured signals rather than manually defined or tuned. This distinction reflects a shift toward automated data processing and scalability for large and heterogeneous datasets. To avoid confusion, the sentence has been restructured, and the discussion in the literature review section has been revised to clarify this point.

4. Table 2 lists numerous correlated features (RMS, variance, standard deviation, energy) that likely exhibit multicollinearity. Including all these features appears arbitrary and may degrade model performance due to redundant information. Additionally, clarification on "spectral features" is needed in this table. The spectral section still computes time-domain features.

Answer: We have carefully revised Table 2 and the corresponding section to clarify the feature definitions and address concerns about multicollinearity. The features originally described as "spectral" were in fact time-domain (temporal) features, as pointed out by the reviewer, and this terminology has been corrected throughout the manuscript.

To address the reviewer's concern regarding redundancy and multicollinearity, a feature correlation analysis was conducted and presented in Figure 4. This analysis revealed two main feature groups exhibiting similar statistical behaviour. Group 1 consists of the RMS and median, which represent the central tendency of the signal. Group 2 assumed the maximum, minimum, amplitude range, variance, energy centre, and signal rate representing variability and extreme values. Features such as energy, kurtosis, higher-order moments, and Shannon entropy showed low sensitivity to damage and were therefore excluded during normalisation and further analysis. Based on the correlation results, only four representative features were selected to construct the global dataset: the RMS, maximum, variance, and amplitude. These features were chosen as representative of their respective groups to avoid redundancy, reduce computational cost, and mitigate the risk of overfitting. This selection ensures that the classifier retains the most relevant discriminatory information while improving efficiency and generalisation capability.

The global dataset consisted of features extracted from each sensor axis (measurement_rows × 48 columns) plus SCADA data. To refine the dataset, a canonical correlation analysis was applied to select the most sensitive features per sensor, reducing the dataset from 48 to four representative features plus SCADA data. This step improved computational efficiency and ensured that only the most informative features were retained. Additionally, sensor relevance was validated by removing the best-performing sensor feature, confirming the robustness of the proposed selection strategy. This explanation was updated in section 2.3 of the revised manuscript.

5. Section 2.2 appears to describe routine data preprocessing rather than a methodological contribution. Furthermore, the overall feature engineering pipeline lacks clear explanation of how the final feature vector is constructed.

Answer: The monitoring framework consists of seven steps including clear identify in the revised pipeline figure (Fig.1), where (1) receiving the acquired data; (2) data processing and organisation; (3) feature extraction, normalisation, and grouping for similarity pattern; (4) unsupervised feature labelling and clustering; (5) feature and sensor selection; (6) data splitting, and ML failure identification and classification; and (7) Fault classification and model evaluation. The final step also outputs the operational failure and identifies the best-performing ML

algorithm based on its performance metric. The novelty associated with the hybrid model and multimodal data, feature and sensor selection, data normalization, and multiple fault classification is presented in a comprehensive set of steps outlining the process. Thus, the steps that have novelty associated with them are detailed in sections 2.2, 2.3, and 3.2.

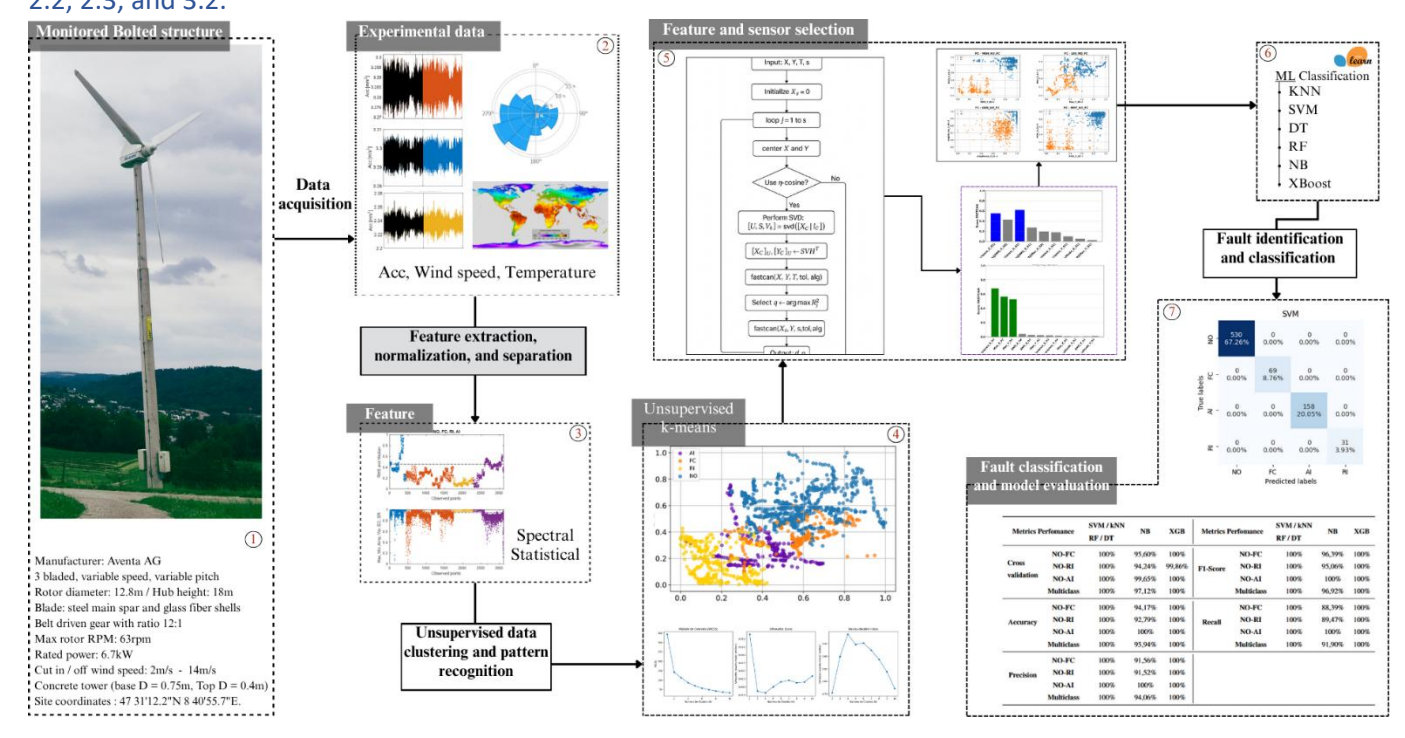


Figure 1. Pipeline of the hybrid machine learning model for fault classification on the Aventa 6.7 kW wind turbine.

The final refined dataset used in step 6 is explained in section 2.3 of the revised manuscript. It is derived from the global dataset, which is assumed to be (measurement_rows \times 48 columns) plus SCADA data. The dataset refinement is performed using canonical correlation analysis (fastcan), which selects the most sensitive features per sensor. In the binary study, the dataset was reduced to 4 representative features, plus SCADA data (measurement_rows \times 6 columns). In the multiclass case, it was reduced to 9 features, plus SCADA data (measurement_rows \times 11 columns). The results of the fastcan for each sensor in the binary and multiclass cases are presented in Figs. 5-10, and detailed information has been added to the revised manuscript.

*A deeper description of the final dataset is given in the answer to question 7.

6. The relative change damage index (Equation 1) lacks theoretical foundation. Why normalize by $max(\Delta f)$ specifically? How does this normalization enhance fault sensitivity? The threshold of 0.6 for feature selection appears arbitrary without statistical justification.

Answer: The initial threshold value of 0.6 was chosen to ensure that the selected features reached at least 60% of the scoring metric. After further evaluation, this threshold was removed from the revised manuscript, and selection was based solely on the highest CCA (fastcan) score. This assumption was consistently adopted for both the binary and multiclass cases.

Regarding the theoretical basis of the proposed relative change (RC) damage index defined in Eq. (1): the normalization by the maximum deviation, $max(\Delta f)$, was deliberately designed to transform each feature into a

dimensionless relative scale ranging from 0 to 1. This operation establishes a consistent reference, corresponding to the feature's maximum observed deviation, against which all other values are compared.

This normalization serves two main theoretical purposes. First, it preserves the intrinsic ordering and proportionality of the data points, ensuring that the feature's dynamic pattern remains unaltered. Second, it rescales the feature space to eliminate the influence of magnitude differences across sensors or feature types, enabling fair comparison among variables with distinct physical units or scales.

Thus, normalizing by the maximum deviation is particularly effective because it defines the undamaged condition as the upper bound (close to unity), while deviations toward zero indicate progressive degradation. This approach enhances fault sensitivity by amplifying subtle variations that would otherwise be numerically insignificant (e.g., 3.280 vs. 3.286) and potentially overlooked by machine learning algorithms.

In summary, the RC normalization provides a physically interpretable and mathematically consistent scaling, ensuring that the features retain their intrinsic dynamic signature while becoming more sensitive and comparable across operational states. This makes the RC-based normalization both theoretically grounded and practically effective for fault detection and classification. The corresponding explanation was added to Section 2.3, and a graphical illustration is now provided in the updated Figure 4.

Added in the revised manuscript:

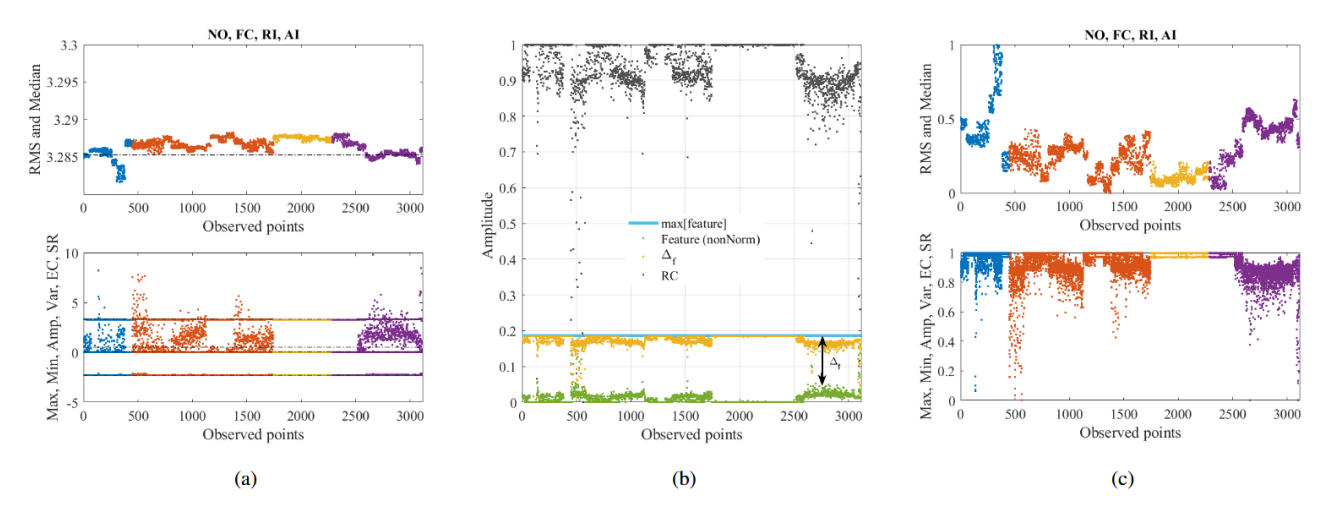


Figure 4. (a) Non-normalized feature grouped by similarity under different operating conditions, NO-blue, FC-orange, RI-yellow, AI-purple colour. (b) Demonstration of the scaling and normalisation on the AMP-feature related to Eq. 1. Scaled and normalised features grouped by similarity under different conditions (c).

This relative change normalization provides a theoretical foundation based on relative scaling and dimensionless feature representation. Figure 4 (a–c) illustrates the process: (a) the non-normalized features, (b) the scaling and normalization applied to the Amp feature (extended to all others), and (c) the normalized features obtained using the proposed relative change technique. The \$RC\$ normalization converts the data into dimensionless features that, prior to normalization, differed only slightly (e.g., 3.280 vs. 3.286), making such variations numerically negligible for machine learning models. Thus, the proposed approach amplifies these small variations while preserving the intrinsic dynamic pattern. Features with values close to unity correspond to undamaged conditions, whereas values approaching zero indicate faults. Hence, the method enhances fault sensitivity and enables consistent comparison across features of different magnitudes, making the damage feature more sensitive to early anomalies under varying operating states.

Features such as energy, kurtosis, higher-order moments, and Shannon entropy exhibited low sensitivity to failures and were excluded during normalisation and analysis. This first supervised analysis revealed two feature groups with

similar behaviour. Group 1 consists of RMS and median (Fig.4 c-Top), while Group 2 comprises maximum, minimum, amplitude range, variance, energy centre, and signal rate (Fig.4 c-Bottom). The formation of two feature groups indicates a high degree of correlation within each group, with RMS and median primarily capturing the signal's central tendency. In contrast, the features of group 2 describe its variability and extremes. Therefore, using all features would introduce redundancy, increase computational cost, and risk overfitting due to the curse of dimensionality. Therefore, selecting only representative features from each group ensures that the classifier retains the essential discriminatory information while improving efficiency and generalisation.

The canonical correlation analysis for sensor ranking (Equations 2-3) requires clearer explanation. The mathematical formulation doesn't clearly translate to practical sensor selection criteria.

Answer: We thank the reviewer for this valuable comment. In the revised version, we have clarified the connection between the canonical correlation formulation and the sensor selection process. Canonical Correlation Analysis (CCA) quantifies the linear relationship between two multivariate datasets: the sensor feature space X and the target (or response) space Y. In the context of sensor ranking, each sensor provides a set of features, and CCA identifies how strongly each sensor's feature set is correlated with the response variable, which represents the system condition or damage state. Similarly, by indicating the best features of each sensor, we can identify the sensor with the highest score for the referee failure. We included the CCA detailed formulation in section 3.2, followed by the pseudocode for fastcan's feature and sensor selection. The included explanation is as follows:

is given in Algorithm 2, which is repeated for each fault diagnosis. The Fastcan method is based on the canonical correlation coefficient (CCA), which is a criterion to measure the linear association between two multivariate random variables. It evaluates the relevance of features with respect to the response matrix. Given the feature matrix $\mathbf{X} \in \mathbb{R}^{N \times n}$ and the response matrix $\mathbf{Y} \in \mathbb{R}^{N \times m}$, the canonical correlation coefficient is defined as

280
$$R_i(\mathbf{X}, \mathbf{Y}) = \max_{\alpha_i, \beta_i} r(\mathbf{X}_C \alpha_i, \mathbf{Y}_C \beta_i),$$
 (2)

where \mathbf{X}_C and \mathbf{Y}_C are column-centred matrices and $r(\cdot,\cdot)$ denotes the Pearson correlation. The projection vectors $\alpha_i \in \mathbb{R}^n$ and $\beta_i \in \mathbb{R}^m$ are obtained by solving the following eigenvalue problems

$$(\mathbf{X}_{C}^{\mathsf{T}}\mathbf{X}_{C})^{-1}\mathbf{X}_{C}^{\mathsf{T}}\mathbf{Y}_{C}(\mathbf{Y}_{C}^{\mathsf{T}}\mathbf{Y}_{C})^{-1}\mathbf{Y}_{C}^{\mathsf{T}}\mathbf{X}_{C}\alpha_{i} = R_{i}^{2}(\mathbf{X}, \mathbf{Y})\alpha_{i},$$

$$(3)$$

$$(\mathbf{Y}_C^{\mathsf{T}} \mathbf{Y}_C)^{-1} \mathbf{Y}_C^{\mathsf{T}} \mathbf{X}_C (\mathbf{X}_C^{\mathsf{T}} \mathbf{X}_C)^{-1} \mathbf{X}_C^{\mathsf{T}} \mathbf{Y}_C \beta_i = R_i^2 (\mathbf{X}, \mathbf{Y}) \beta_i.$$
 (4)

285 The eigenvalues $R_i^2(\mathbf{X}, \mathbf{Y})$ correspond to the squared canonical correlation coefficients, while α_i and β_i are the canonical weight vectors that define the canonical variates $\mathbf{X}_C\alpha_i$ and $\mathbf{Y}_C\beta_i$. There are at most $\min(n,m)$ non-zero canonical correlation coefficients $R_1(\mathbf{X}, \mathbf{Y}), \dots, R_{\min(n,m)}(\mathbf{X}, \mathbf{Y})$. The overall criterion for feature selection is the sum of squared canonical correlations (SSC)

$$SSC(\mathbf{X}, \mathbf{Y}) = \sum_{k=1}^{\min(n, m)} R_k^2(\mathbf{X}, \mathbf{Y}). \tag{5}$$

290 To accelerate computation, the SSC can be reformulated using two equivalent decompositions: (i) the h-correlation form (valid when $N \le n + m$),

$$SSC(\mathbf{X}, \mathbf{Y}) = \sum_{i=1}^{n} \sum_{j=1}^{m} r^{2}(w_{i}, v_{j}),$$
(6)

where $\{w_i\}$ and $\{v_j\}$ are orthogonal bases of the feature and response spaces; and (ii) the θ -angle form (valid when N>n+m),

295
$$SSC(\mathbf{X}, \mathbf{Y}) = \sum_{i=1}^{n} \sum_{j=1}^{m} \cos^{2}(\angle(w_{i}, v_{j})),$$
 (7)

where the canonical correlations are expressed as squared cosines of the principal angles between the subspaces of X and Y. In the greedy selection step, the next feature x_{ri} is chosen to maximise the incremental SSC

$$d = \arg\max_{i} \sum_{k=1}^{\min(p+1,m)} R_k^2((\mathbf{X}_s, x_{ri}), \mathbf{Y}), \tag{8}$$

where \mathbf{X}_s denotes the already selected features. This formulation allows efficient feature ranking by reducing computational complexity while preserving the theoretical properties of canonical correlation analysis. This process involves looping through the features for each sensor in an interaction. In sequence, a similar procedure is performed for sensor ranking, with the feature matrix defined as $\mathbf{X}_s \in \mathbb{R}^{S \times s}$, where \mathbf{X}_s contains the highest ranking feature(s) of each sensor.

7. Table 4 reports perfect results for SVM/kNN/RF/DT, yet the text states only SVM achieves perfect performance. This contradiction requires clarification. How do you justify these perfect accuracy claims, and have you conducted statistical validation? Such results typically suggest potential overfitting.

Answer: A deeper investigation into the sensitivity of the ML algorithms and the possible cause of the perfect metrics was introduced. Therefore, all results were checked and validated in the revised manuscript. The model employs a multiphysic dataset, considering structural and environmental information. At first, the general dataset serves as input to the k-means for pattern recognition and labelling.

The environmental information, consisting of the daily average temperature and wind speed, was provided by the turbine's owner in such a configuration. We identify that when the dataset organisation assumes Features-SCADA and then uses k-means for labelling, the SCADA features are highly correlated and influence the k-means grouping. Therefore, masking the failure's sensitivity. Furthermore, we implemented four data organization methods to demonstrate the influence of data arrangement and to indicate an optimal dataset configuration.

We demonstrated the impact of the dataset arrangement, the influence of the environmental conditions, and sensors on the performance metrics of the ML models. Also, the statistical validation was performed in all cases and demonstrated in the cross-validation metric (Fig. 11a- d (last column)). The following action was updated in the revised manuscript.

Included in the manuscript:

The final refined dataset organization is a crucial step in enabling machine learning algorithms to classify operational failures accurately. The deployed dataset exhibits a multimodal nature, integrating structural, temperature, and wind velocity information. The structural information is directly obtained from the accelerometers, which capture the system's physical response and potential failure signatures. In contrast, temperature and wind speed data are obtained from the SCADA system and represent indirect but relevant variables that influence the dynamic behaviour measured by the accelerometers, although they do not directly describe the damage dynamics. The final dataset is organized into four configurations, which are evaluated and their relevance demonstrated in the section 4.

- **Fe-kms-Sc:** dataset composed of the selected features (Fe) extracted from the accelerometer time signals, followed by the SCADA data (Sc), and beelining provided by the k-means clustering (kms).
- Fe-Sc-kms: dataset including the selected features, the SCADA data, and the corresponding k-means labels.
- **Fe-kms:** dataset including only the selected features and the k-means labels, without incorporating the SCADA information.
- **Fe-kms-LoseSensor:** dataset including the selected features excluding those obtained from the most sensitive sensor identified by the Fast CCA method, together with the k-means labels and SCADA data. This configuration simulates the loss of the most sensitive sensor in each analysis scenario.

The k-means labelling of the datasets Fe-kms-Sc and Fe-kms-LoseSensor is applied exclusively to the features that contain the most relevant physical information about the damage. The SCADA data are then organized by the corresponding day and hour for each feature sample. This ensures that the SCADA records follow the same row reordering imposed by the k-means clustering, while preserving the correct temporal (day and hour) correspondence between the SCADA measurements and the related accelerometer data.

The results for each dataset are shown in the new Figure 10, which compares the ML metrics for each algorithm and dataset.

Included in the manuscript:

The ML models were tested on the Fe-kms-Sc, Fe-Sc-kms, Fe-kms, and Fe-kms-LoseSensor datasets to assess the influence of environmental dependencies (SCADA data) and the sensitivity of each sensor in failure evaluation. The metrics for the **Fe-Sc-kms** dataset, shown as black (\$\ast\$) in Fig.~\ref{metrics}(a-d), indicate that, except for the NB classifier, all ML models achieved 100\% accuracy. Such perfect performance across multiple models can suggest potential issues like data leakage, overfitting, or improper dataset splitting. However, cross-validation with multiple random partitions was performed to ensure statistical robustness. In this case, the consistently high accuracy reflects the physical consistency and strong discriminative power of the selected features rather than methodological flaws.

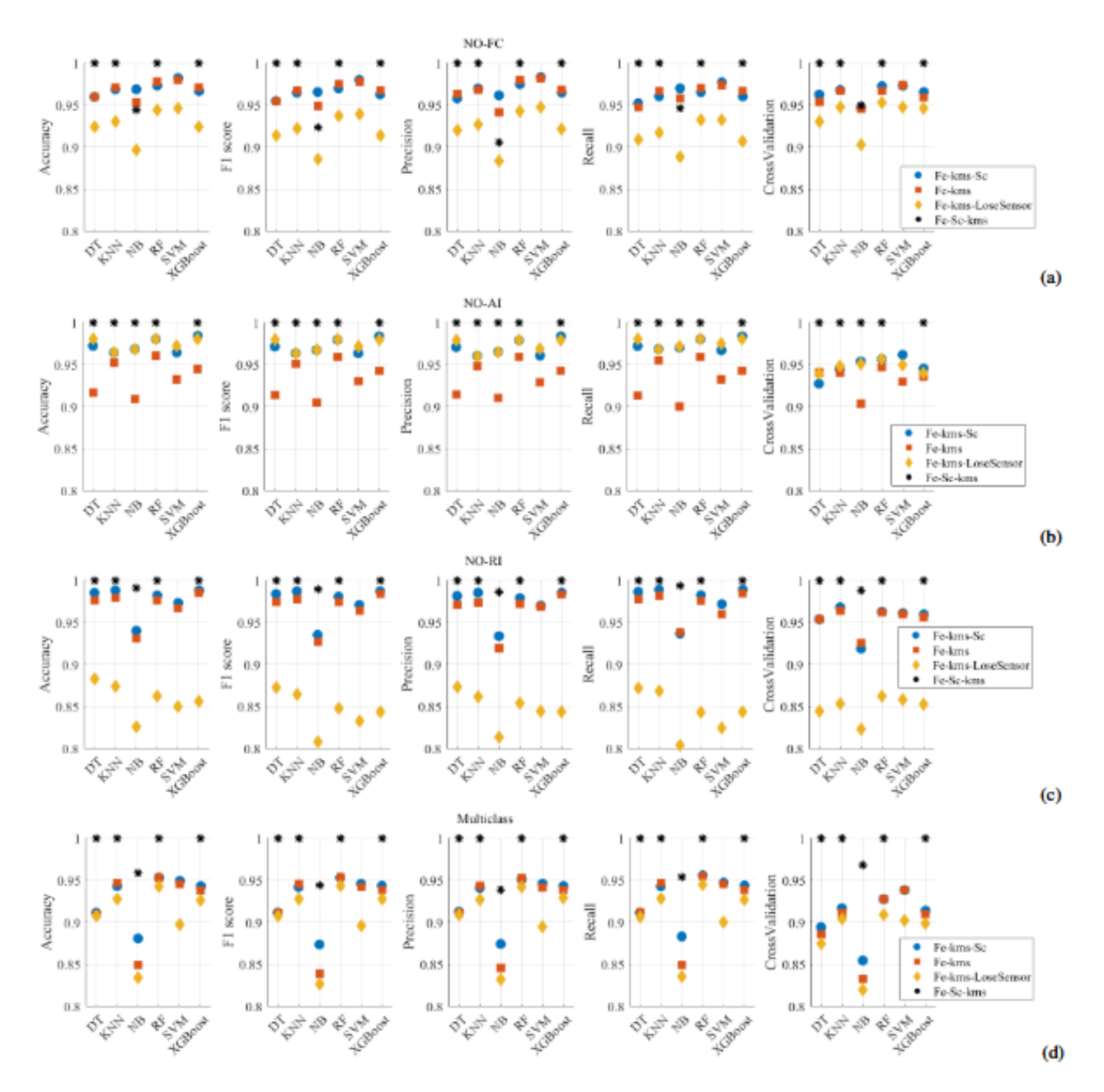


Figure 10. Comparison of the metrics (accuracy, F1-score, precision, recall, and cross-validation) for the six ML algorithms and each arranged final dataset. (a) Binary NO-FC, (b) Binary NO-AI, (c) Binary NO-RI, and (d) multiclass failure study cases

The k-means clustering results and associated metrics also reveal clear class separation. The feature scores derived from the CCA, which quantify the linear association between the selected features and the k-means clusters (Fig.10), highlight the strong correlation between SCADA data and the structural sensors (accelerometers). The SCADA system provides environmental variables, such as daily temperature and wind speed, but lacks important structural information more directly related to damage states. In the Fe-Sc-kms dataset configuration, both features and SCADA inputs are used in the k-means clustering, which is predominantly influenced by the SCADA parameters. Therefore, the perfect ML metrics are attributed to dataset bias, where the models primarily classify failure conditions based on environmental variations rather than the structural response itself.

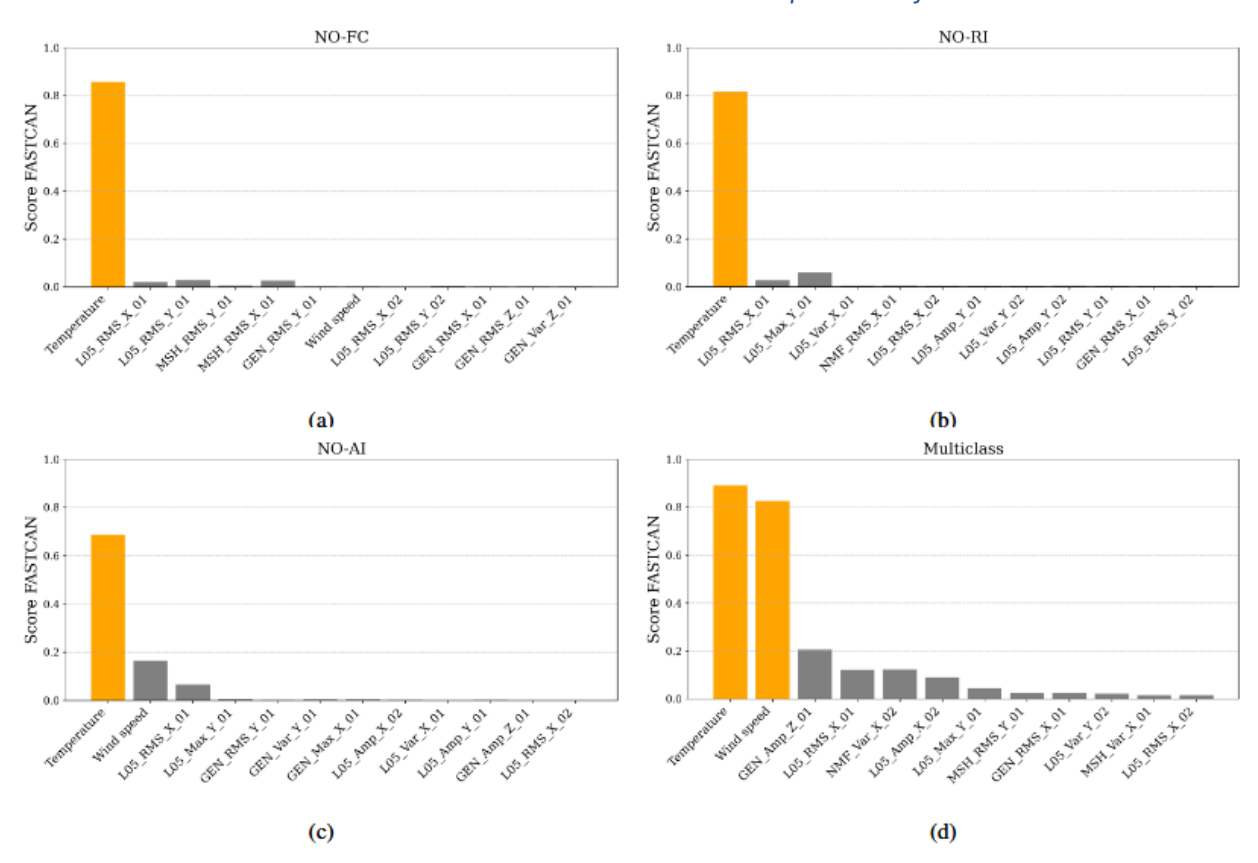


Figure 11. Feature score of the Fe-kms-Sc dataset for (a) NO-FC, (b) NO-RI, (c) NO-AI, and (d) multiclass.

The ML models' metrics for the **Fe-kms-Sc** dataset, shown as blue \$\bullet\$ in Fig.11(a-d), indicate the sensitivity of the ML models to the damage. The k-means is performed on the structural features, and the SCADA follows its data reorganization, but it is not directly considered in the k-means labeling. For the binary case, the model's metrics range from 0.93 to 0.99. The SVM model reached 0.98 on the NO-FC case, XGBoost reached 0.98 for NO-AI, and XGBoost reached 0.99 for NO-RI. Multiclass case varied from 0.86 given by NB to 0.955 by RF.

The SCADA data are not included in the **Fe-kms** dataset, shown as orange-\$\blacksquare\$ in Fig.11(a-d). The performance metrics reached 0.98 with the SVM model for the NO-FC case, 0.955 with RF for the NO-AI case, 0.98 with XGBoost for the NO-RI case, and 0.95 with RF in the multiclass analysis. When the most sensitive sensor for each failure case was removed from the **Fe-kms-LoseSensor** dataset (yellow \$\bLozenge \$), performance metrics decreased, except for NO-AI, indicating the importance of this sensor's information for monitoring accuracy and model performance. This also reinforces that the most sensitive sensor is typically located near the damage site. In the NO-AI case, all sensors were positioned on the nacelle and tower. Although these sensors can capture the dynamic effects of blade aero-imbalance, they are distant from the local damage, which reduces their sensitivity. Consequently, the sensor group primarily captured global structural responses to the fault rather than local damage effects, explaining the performance variation when one of the sensors was removed.

8. Figures 3b-c demonstrate clear environmental dependencies, but the model's ability to **distinguish between environment-induced changes and actual failures remains unvalidated.**

Answer: Aside from figure 3b-c, the new results presented in Figure 10 a-d confirm that environmental parameters (from SCADA data) strongly influence the model's output when included in the dataset configuration. This is evident in the Fe-Sc-kms dataset, where all models achieved near-perfect accuracy due to the dominance of environmental features, primarily temperature and wind speed. However, to isolate and validate the model's ability to distinguish true structural failures from environmental variations, additional datasets were tested.

In the Fe-kms configurations, the SCADA data were either excluded or aligned only with the structural features, allowing the models to rely primarily on vibration-based indicators. These configurations showed lower, yet physically consistent, performance (metrics around 0.93), demonstrating that the models can indeed detect failure-induced changes but without the intrinsic parameter of environmental fluctuations. However, when SCADA data were correctly incorporated into the analysis, the Fe-kms-Sc dataset, which integrates structural features with aligned but non-dominant environmental information, yielded the most physically consistent and discriminative performance for wind turbine failure classification.